Contents lists available at ScienceDirect

Knowledge-Based Systems

A local fuzzy thresholding methodology for multiregion image segmentation

Santiago Aja-Fernández *, Ariel Hernán Curiale, Gonzalo Vegas-Sánchez-Ferrero

LPI, ETSI Telecomunicación, Universidad de Valladolid, Spain

A R T I C L E   I N F O

A B S T R A C T

Thresholding is a direct and simple approach to extract different regions from an image. In its basic formulation, thresholding searches for a global value that maximizes the separation between output classes. The use of a single hard threshold value is precisely the source of important segmentation errors in many scenarios like noisy images or uneven illumination. If no connectivity or closed objects are considered, the method is prone to produce isolated pixels. In this paper a new multiregion thresholding methodology is presented to overcome the common drawbacks of thresholding methods when images are corrupted with artifacts and noise. It is based on relating each pixel in the image to different output centroids via a fuzzy membership function, avoiding any initial hard decision. The starting point of the technique is the definition of the output centroids using a clustering method compatible with most thresholding techniques in the literature. The method makes use of the spatial information through a local aggregation step where the membership degree of each pixel is modified by local information that takes into account the memberships of the surrounding pixels. This makes the method robust to noise and artifacts. The general formulation of the proposed methodology allows the design of spatial aggregations for multiple applications, including the possibility of including heuristic information via a fuzzy inference rule base.

© 2015 Elsevier B.V. All rights reserved.

1. Introduction

Thresholding is one of the most direct and simple approaches to image segmentation. It is an effective method as long as the image shows well defined areas and the gray levels are clustered around distant values with minimum overlap. It also has been used to provide an initial estimation or a prior to more complex segmentation methods (techniques based on snakes, level-sets or active contours need an initial segmentation, that can be manually done or obtained via thresholding [1,2]), to provide masks of regions of interest [3], or even as a technique to detect motion in surveillance environments [4,5]. Thresholding is also extensively used in the medical imaging field, where images are composed by several tissues, represented by their gray levels [6]. The arrangement of these tissues or organs inside the image is usually clearer than the arrangement of objects in a natural scene image, hence the using of specific thresholding techniques.

Image thresholding techniques are well known, and some of the most used methods date from the 70s, such as Otsu's method [7,8].

In its basic implementation, thresholding methods search for a global threshold value that somehow maximizes the separation between classes in the final result. However, regardless of the method chosen to find the separation between classes, the use of a single hard value is known to be the source of important segmentation errors when dealing with noisy images, uneven illumination and soft transitions between gray levels [9–11]. The main drawback of this global threshold approach is due to it being *pixel* oriented rather than *region* oriented, and therefore those pixels having the same gray level value will always be segmented into the same class. If no connectivity or closed objects are considered, the method is prone to produce isolated pixels.

Thus, despite being a long standing problem, these issues have not been resolved, and new approaches are required to solve different configuration of signal and images; see some surveys of them in [9,12–15]. In the first one [9], authors classify thresholding methods into six main categories:

1. Methods based on the shape of the histogram [7,8].
2. Clustering-based methods [16–21].
3. Entropy-based methods [22–24].
4. Local methods, that adapt the threshold value on each region based on local features [25,26].

* Corresponding author.
E-mail addresses: sanaja@tel.uva.es (S. Aja-Fernández), ariel@lpi.tel.uva.es (A.H. Curiale), gvegsan@lpi.tel.uva.es (G. Vegas-Sánchez-Ferrero).

5. Object attribute-based methods that search a measure of similarity between gray-levels and objects, such as fuzzy shape similarity.
6. Spatial methods that use higher-order probability distribution and/or correlation between pixels [11].

The first three methodologies comprise the main *tradition* behind thresholding methods: the search for a global threshold that allows us to divide the image into two or more regions. Methods proposed in the literature can grow in complexity in the pursuit of the optimal threshold but ultimately, the final segmentation will only depend on the gray level of each particular pixel. The final classification is done pixelwise. Note that most of the algorithms based on fuzzy measures [27–33] fall into these categories. On the other hand, local methods assume that different areas in the image require different thresholds. This is the case for images with uneven illumination, in which objects are not totally represented by absolute gray values.

All these methodologies will fail in the case of images corrupted by noise, where the gray levels of each object are spread and merged due to the noisy distortions. Attribute-based methods are a good alternative, as long as we have key information about the objects in the scene. Finally, spatial methods take into account possible relations between pixels. The idea behind them is the fact that pixels belonging to the same object will have a certain degree of connectivity, i.e., the presence of isolated pixels is unlikely and there is a strong relation between a pixel and its neighborhood.

Note that these six categories can be merged into three practical methodologies:

1. Methods that calculate a global threshold for the whole image.
2. Methods that use an adaptive local threshold.
3. Methods that use spatial local information for classifying the pixels.

In this paper we propose a new thresholding methodology that takes advantage of the main features of the last two categories:

- The membership degree of a particular pixel in a class is spatially related with the membership of its surrounding neighbors.
- The final thresholding will take into account the local membership in each of the classes, which implicitly makes the threshold locally variant.

The main contribution of this paper relies on Fuzzy Sets Theory and Fuzzy Logic [34]. Fuzzy logic is known to be a very flexible tool in classification problems where imprecise knowledge or not-well-defined features have to be used. In addition, fuzzy logic is also a natural selection where information has to be retrieved from linguistic statements. It has been widely used in the field of systems control [35], but there are also a great amount of applications in the image processing field [36–38]. In the last 20 years, many methods based on fuzzy logic and fuzzy measures [39,40] have been proposed for image thresholding. They are mainly focused on the search for the optimum threshold using fuzzy measures, buy many times they do not take into account spatial information. Some of the techniques used comprised fuzzy clustering [41,42], modified versions of fuzzy clustering methods [19,21], fuzzy measures [27,43,30,44], optimization of fuzzy compactness [45], fuzzy entropy [46] and the interpretation of thresholds as type II fuzzy sets [33,32]. Parallel with fuzzy measures, other soft computing methods have arisen, such as the heuristic methods based on ant, bees and bacteria colonies [47–49].

In this paper we propose a new methodology which differs from those approaches in the literature. The starting point is the idea

that the membership of a pixel in a particular class or object will be highly correlated with the membership in that class of the surrounding pixels. To take into account this local spatial information we propose the use of fuzzy sets: a pixel will be assigned to the different classes of a multiregion segmentation through a fuzzy membership function. The traditional hard assignment (i.e. a pixel belongs or does not belong to an output class) is replaced by a soft assignment, following the basic theory of fuzzy sets.

The paper is organized as follows: Section 2 presents the new thresholding methodology proposed. Results and comparison with another methodologies and methods are shown in Section 3. Conclusions are presented in Section 4.

2. Multiregion fuzzy thresholding

2.1. Motivation and purpose

The main limitation of global thresholds is that pixels having the same intensity levels will always be segmented into the same class. This may lead to misclassification in images corrupted by noise or uneven illumination. To overcome this problem, information about the behavior of the spatial surroundings of each pixel must be considered. This spatial information can be taken into account using very different methods, each one of them generating a different output segmentation. Most used methods are those we can call *blind methods*: methods that *clean* the segmented image using local processing but without any prior information of the image structure, object distribution, nature of noise, etc. These methods only make use of the segmented values. Some common examples are the median filtering and morphological operations to remove isolated pixels.

To motivate use of the local information, see for instance the image in Fig. 1. A pixel has been classified as belonging to the Class 3 (red). In a 3×3 neighborhood around the pixel we can check that this pixel is an isolated value, probably generated by noise. The *correction* to this misclassification can be done using information about the image (such as the model of noise, the classification probability, the distance to the centroid) or just using spatial or morphological operations. Note that if we use a median filter over that neighborhood, the pixel will now be classified as Class 1 (blue). Similar results can be found using a filling algorithm. In those cases, important information about the image is missing. If we check the distance to the centroids, we realize that the pixel is 0.52% Class 3 and 0.48% Class 2, and it has been classified as 3 by a small range. In a noisy image, it is very likely that this pixel belongs to Class 2, and is unlikely to belong to Class 1. In what follows we will be using this idea of taking into account the local properties to improve the classification methodology.

We propose a new thresholding methodology to make a multiregion segmentation of the different areas within an image. To that end, we will follow a fuzzy assignment classification that will follow the philosophy behind many fuzzy-based approaches in the literature [27–31], but it will be complemented with a spatial aggregation step that will take advantage of the soft classification and the spatial relations. Our *fuzzy thresholding* methodology will assign a membership degree to every pixel for each of the output classes, rather than to a traditional hard thresholding. The membership degree of each pixel is then modified using local information following some aggregation scheme and some fuzzy rules set beforehand. The aggregation method is to be specifically designed for each particular application, although some examples will be given. The inclusion of this aggregation step will be a great advantage when dealing with noisy images.

Finally, note that the methodology is compatible and complementary to some of the methods already proposed in the literature,
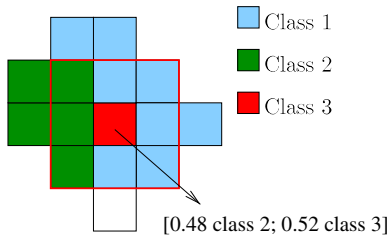
Fig. 1. Example of classification of noisy pixel.

since the starting point is precisely a fuzzy assignment of pixels to classes.

2.2. Proposed thresholding methodology

Let $I(\mathbf{r})$ be an image with L different regions we want to extract via thresholding, in order to obtain a segmented image $M(\mathbf{r})$, so that

$$M(\mathbf{r}) = g_s\{I(\mathbf{r})\}$$

where $g_s\{\cdot\}$ is the segmentation method that can be considered a function that maps the N_I levels of gray of image $I(\mathbf{r})$ into L values, i.e. $g_s : N_I \to L$ with $L < N_I$.

To carry out the segmentation, the proposed methodology assumes that every pixel in the image $I(\mathbf{r})$ will have a degree of membership in each of the L regions. That membership will be modeled using fuzzy membership functions. In what follows, we will denote $\mu_l(x), l = 1, \ldots, L$, as the fuzzy membership function of the lth area. Spatial aggregations can therefore be applied into the *membership plane* to take into account the relation between adjacent pixels prior to obtain the final segmentation.

The methodology, surveyed in Fig. 2, comprises five steps. Since the proposal is a *methodology* and not a closed algorithm, in each of the steps we provide alternative implementations of the methods. The election of any choice will depend on the kind of data and the particular features of the segmented image. Some of the proposed choices were tested and will be described in the experiments section. The five steps of the thresholding methodology are as follows:

(1) Extraction of the centroids: The different areas in which the image will be segmented are defined using L centroids. Typically, as previously stated, $L < N_I$. The number of centroids can be manually set beforehand by the user or the algorithm can be automatically tuned to search for the optimum number of regions. Many of the methods proposed in the literature for traditional thresholding may be used here in this first step, specially those based on clustering [16,17,50] or entropy of the histogram [23,24].

(2) Definition of fuzzy membership functions: A fuzzy membership function $\mu_l(x)$, with $l = 1, \ldots, L$ is associated to each of the classes linked to the previously defined centroids. There are two possible ways to define the membership functions:

(a) *From the histogram of the image, $h(I)$.* This method follows the classical approach for multiregion thresholding, in which the main levels within the image are extracted from the histogram, $h(I)$. A sum of L weighted distributions is fitted to $h(I)$:

$$h(I) \approx \sum_{l=1}^{L} \omega_l \cdot p_l(x; \theta_l) \tag{1}$$

with $p_l(x; \theta_l)$ a probability density function defined by the set of parameters θ_l, and ω_l are weights which satisfy that $\sum_l \omega_l = 1$. The fitting can be done using a minimization algorithm, such as minimum mean square error (MMSE):

$$\arg\min_{\theta_l, \omega_l} \left| h(I) - \sum_{l=1}^{L} \omega_l \cdot p_l(x; \theta_l) \right|^2. \tag{2}$$

Typically Gaussian distributions are good candidates for $p_l(x; \theta_l)$ to represent the histograms. However, some modalities of medical imaging may benefit by using alternative distributions. MR data, for instance is known to follow a Rician distribution [51,52] that can be accurately approximated by a Gaussian for high Signal-to-Noise Ratios. Ultrasound data, on the other hand, have been described using a myriad of distributions, such as Rayleigh, K or homodyned-K. Lately in [53] authors show that, due to the interpolation on the data, the histogram may be represented more accurately by a mixture of Gamma distributions. Therefore, in those applications, a Gamma is a better candidate for $p_l(x; \theta_l)$.

Our intention is to use *membership* instead of *probability* values. To that end, we use the information of the histogram to model the fuzzy sets that will provide this membership information. The simplest way would be using Gaussian membership functions (MF), such as the ones in Fig. 3(b). Note that the transition from probabilities to membership comes with a transformation of the first and last sets, and a normalization of the weights.

Although a natural transition, Gaussian MFs have some problems related to Fuzzy Sets Theory [54,55]: they are not *consistent* and the intersection of the sets is in a value smaller than 0.5. In order to work properly, we require the fuzzy sets to be:

(i) A complete partition: $\forall x, \exists \mu_l(x), 1 \leqslant l \leqslant L$, such that $\mu_l(x) > 0$.
(ii) Consistent: if $\mu_l(x_0) = 1$, then $\mu_k(x_0) = 0 \; \forall k \neq l$.
(iii) Normal: $\max(\mu_l(x)) = 1$.
(iv) The intersection between adjacent fuzzy sets is $\mu_l(x_0) = \mu_{l+1}(x_0) = 0.5$.

To that end, we choose to use Pseudo Trapezoid-Shaped (PTS) [54] membership functions, as depicted in Fig. 3(c). Alternative methodologies to obtain the MFs from the histogram can be found in [56–58].

(b) *From the centroids, leaving aside histogram information.* If PTS-MFs are used, all the information of the histogram can be left aside, since the sets in Fig. 3(c) can be built directly from the centroids values extracted in the previous step. This is an advisable solution for general purpose segmentation or when there is no precise knowledge about the distribution of objects or tissues in the image.

In what follows, the central fuzzy sets are selected to be triangular (a particular shape of PTS). However, more complex shapes may be adopted, as trapezoid MFs, taking into account the variance of the fitted Gaussian.

The output of this step will be the MFs that describe each of the output sets, $\mu_l(x), 1 = 1, \ldots, L$.

(3) Assigning membership to each pixel: The membership of pixel $\mathbf{r}$ in the image $I(\mathbf{r})$ in the l-th class is given by $\mu_l(I(\mathbf{r}))$. Using PTS MF as previously defined, note that

$$\sum_{l=1}^{L} \mu_l(I(\mathbf{r})) = 1.$$

At this point, a first thresholding of the image could already be done:

$$M(\mathbf{r}) = \arg\max_l \{\mu_l(I(\mathbf{r}))\} \tag{3}$$

with $M(\mathbf{r})$ the output thresholded image. However, this way we are not taking advantage of the information of the neighborhood, and
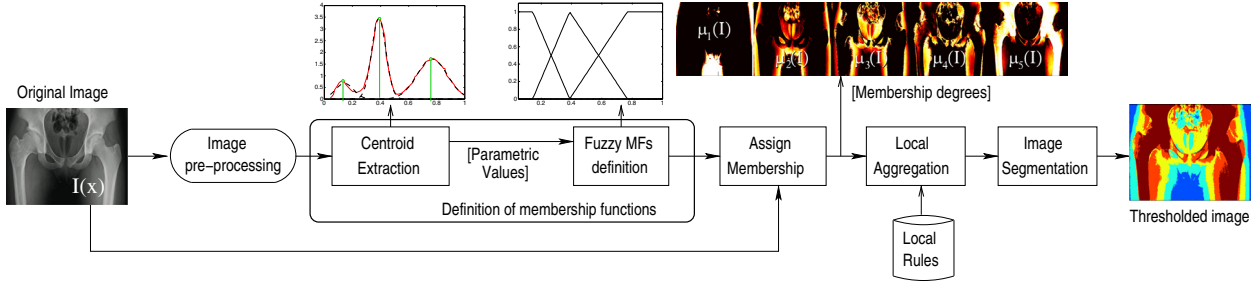
Fig. 2. Pipeline of the multiregion fuzzy thresholding methodology described in the paper.

(a) Histogram with fitted Sum of Gaussian

(b) Gaussian membership functions

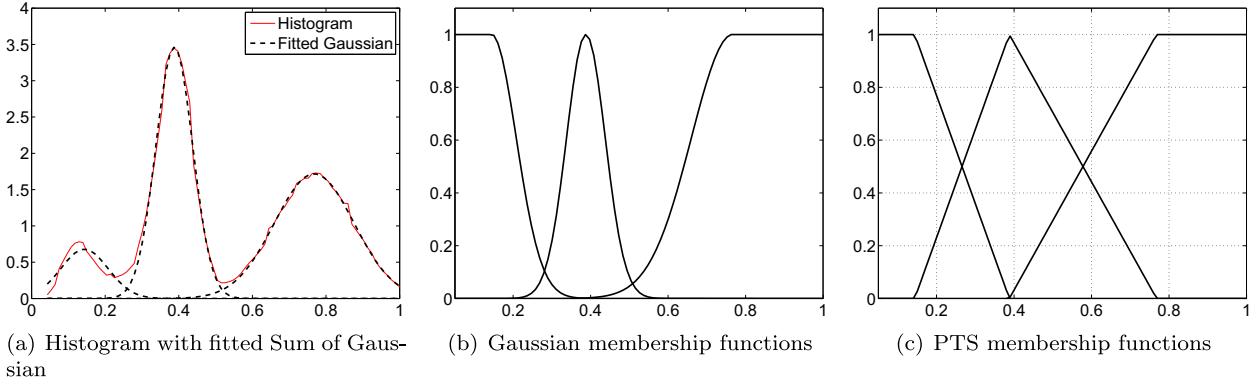(c) PTS membership functions

Fig. 3. From probability to membership: (a) (Normalized) histogram of the image $h(I)$, with three weighted Gaussian, $p_l(x)$ fitted using MMSE. (b) From $p_l(x, \theta)$, three fuzzy sets with Gaussian membership functions are created. (c) Alternatively, from $p_l(x, \theta)$ three fuzzy sets with PTS membership functions are created.

the results will be strongly dependent on the method selected for the centroid search.

The output at this stage, for each pixel, will be a vector of memberships:

$$\boldsymbol{\mu}(I(\mathbf{r})) = [\mu_1(I(\mathbf{r})) \quad \mu_2(I(\mathbf{r})) \quad \cdots \quad \mu_L(I(\mathbf{r}))]$$

If PTS MFs are selected, only 2 of the elements of each vector would be different from zero.

(4) Local information aggregation. In this step, spatial information will be taken into account before obtaining the final segmentation. This step is the main contribution of the proposed methodology. The versatility of fuzzy logic allows us to design many different ways to consider the influence of the neighborhood from the $\boldsymbol{\mu}(I(\mathbf{r}))$ degrees previously defined. In what follows we propose an aggregation based solution, suitable for general image thresholding.

If we consider a neighborhood $\eta(\mathbf{r})$ centered around a pixel $\mathbf{r}$, we can use the membership values $\boldsymbol{\mu}(I(\mathbf{r}))$ of all the pixels in $\eta(\mathbf{r})$ to better classify the image into regions. To that end we propose a local aggregation of values:

$$\boldsymbol{\mu}^{\mathcal{S}}(I(\mathbf{r})) = \underset{\mathbf{s} \in \eta(\mathbf{r})}{\mathrm{agg}} \{\boldsymbol{\mu}(I(\mathbf{s}))\} \tag{4}$$

where agg$\{\cdot\}$ is an fuzzy aggregation in a neighborhood $\eta(\mathbf{r})$. The purpose of this function is the modification of the original membership functions $\mu_l(I(\mathbf{r}))$ when local information is taken into account. One important feature of this operation is that we work in the membership space, not over the image or over the final segmentation. Different aggregations based on the pixels in the neighborhood can be defined, properly tuned to the desired output. Some neighborhood based rule-sets for fuzzy image processing have been previously proposed in the literature, see for instance [59,60,38,61], that could be easily adapted to the proposed scheme. Fuzzy morphological operators, like those described in [37,57] can also be

applied. In the following we propose some aggregations for general purpose image thresholding.

(a) *Median Aggregation (MedAg):* The memberships of each of the pixels in $\eta(\mathbf{r})$ are aggregated using the median operator

$$\mu_l^{\mathcal{S}}(I(\mathbf{r})) = \underset{\mathbf{s} \in \eta(\mathbf{r})}{\mathrm{median}} \{\mu_l(I(\mathbf{s}))\} \tag{5}$$

Note that the neighborhood $\eta(\mathbf{r})$ can be oriented in order to better find structures in one particular direction.

(b) *Average aggregation (AvAg):* We define an averaging of each MF as

$$\mu_l^{\mathcal{S}}(I(\mathbf{r})) = \sum_{\mathbf{r}_i \in \eta(\mathbf{r})} \omega_i \cdot \mu_l(I(\mathbf{r}_i)) \tag{6}$$

with ω_i the weights of the pixels considered. One possible definition would be a square uniform neighborhood so that $\omega_i = 1/|\eta(\mathbf{r})|$, with $|\eta(\mathbf{r})|$ the size of the considered neighborhood. Note that when using PTS MFs, only two MFs $\mu_l(I)$ will have values different from zero. Thus, the averaging will highly reduce the value of those isolated pixels, while keeping the values of the homogeneous areas.

(c) *Iterative averaging aggregation (IterAg):* In order to better find structures, we can define an iterative procedure that averages the membership space. Since a tradeoff between structure finding and smoothing must be considered, a small averaging window must be defined:

$$h = \frac{1}{3} \begin{bmatrix} 0 & 0.5 & 0 \\ 0.5 & 1 & 0.5 \\ 0 & 0.5 & 0 \end{bmatrix}.$$

The aggregation is then defined as

$$[\mu_l(I(\mathbf{r}))]_{t+1} = [\mu_l(I(\mathbf{r}))]_t * h, \tag{7}$$

with $*$ being spatial convolution and $t = 0, \ldots, T$ the number of iterations. Finally

$$\mu_l^S(I(\mathbf{r})) = [\mu_l(I(\mathbf{r}))]_T.$$

(d) *Absolute Maximum (AbMax):* The membership of each of the pixels in $\eta(\mathbf{r})$ is aggregated using the maximum operator:

$$\mu_l^S(I(\mathbf{r})) = \max_{\mathbf{s} \in \eta(\mathbf{r})}(\mu_l(I(\mathbf{s}))). \tag{8}$$

We have avoided any kind on implementation based on rules and fuzzy decision, as some heuristic is always involved. However, for a particular implementation (for instance to threshold bones in radiograph images to search for a particular disease, or for text identification) one can think on using alternative spatial filters with fuzzy rules, such as the Russo's FIRE operators [37].

(5) Image segmentation. The last step is to calculate the final segmented image from the modified membership functions. We propose using the maximum operator:

$$M(\mathbf{r}) = \arg\max_l \left\{ \mu_l^S(I(\mathbf{r})) \right\} \tag{9}$$

although other defuzzification and centroid calculation methods can be used [34].

3. Experiments and Results

We experimentally tested the methodology proposed in this paper. Throughout this section, the images used are those shown in Fig. 4.

First, we analyze the influence of the centroid extraction method on the final segmentation. As previously stated, different methods can be used in order to extract the L centroids that will determine the multiple regions within the image. The determination of these centroids is key to the accuracy of the method. However, the choice of the most suitable method will depend on the final application. Most of the clustering and thresholding methods in the literature can be used for this task. For the sake of illustration, three different simple approaches are considered:

1. The centroids are selected from the L most relevant maxima of the histogram $h(I)$, and PTS membership functions are created from this centroids.
2. The centroids are obtained from the fitting of L Gaussian distributions to the histogram of the image $h(I)$ following Eq. (2). Gaussian MF are created from the results.
3. A clustering method (fuzzy c-means [50]) is used in order to obtain L centroids. PTS membership functions are created from these centroids.

For each method, two different inputs are considered for the centroid calculation: the unprocessed image, $I(\mathbf{r})$ and a smoothed version, using a Gaussian kernel with $\sigma = 1.5$. From the MFs a simple segmentation is done by using the maximum membership in Eq. (3). For this experiment, no local aggregation is done and $L = 5$ regions are considered. Images in Fig. 4(a) are used. Results are shown in Fig. 5.

From the results we can see the great influence of the centroid selection method over the final segmentation. For this particular case, the Gaussian MFs, Fig. 5 shows a less robust behavior and they greatly benefit from the smoothing of the data. Clustering, Fig. 5(c) and (f), appears to be a robust method which goes well with the PTS memberships, and it is rather invariant to the smoothing in the image. The use of the maxima of the histogram, Fig. 5(a) and (d), also shows a good behavior, though it is more sensitive to image smoothing. In any case, note that all the methods succeed in properly separating the cell from the background, and even in

locating important structure inside the cell. In our comparisons with well-known thresholding techniques, we use the fuzzy c-means clustering method.

Second, we analyze the behavior of the different aggregations proposed. To that end, we will use the following data: the cell in Fig. 4(a) (corrupted by additive Gaussian noise with $\sigma = 10$ and $\sigma = 20$) and the radiographic image in Fig. 4(h). All pixel ranges are [0, 255]. In all the methods $L = 5$ sets are considered. Results are given in Figs. 6 and 7.

From Fig. 6, we can raise some interesting issues about the behavior of the different methods. Note that all succeed in the task of properly identifying the regions within the image, despite the noise. When the noise increases, MedAg fails to properly identify the edges, since it keeps some of the noisy pattern, while AvAg and IterAg show a very accurate segmentation with connected objects. The AbsMax works properly for the original image but shows undesired effects in noisy data. These differences are less obvious when a non-noisy image is considered, like the finger in Fig. 7. There, all the methods show a similar behavior with subtle differences.

Third, we compare the proposed method with some well-known thresholding techniques. To that end, we have selected some classic algorithms, fuzzy-based thresholding techniques and methods that take into account spatial information. We consider these methods to be representative of the state-of-the-art thresholding techniques:

1. Otsu hard thresholding method for 2 regions (Otsu) and an extension for N regions (Otsu-N) [7,8].
2. Fuzzy c-means (FCM): The segmentation is done using the clustering method proposed in [50]. The algorithm clusters objects into c partitions, attempting to find the centroids of natural clusters in the data. To do that, the algorithm minimizes the intra-cluster variance through a squared error function. The number of centroids is required as a parameter of the method.
3. The Iterative Thresholding Segmentation (ITS) algorithm proposed in [10]. We choose this method since it was originally for segmentation of very noisy cell images. The initial threshold is iteratively adjusted based on local information, obtaining a final image less sensitive to noise. Only two output sets are considered.
4. Maximum *a posteriori* spatial probability segmentation (MASP), as proposed in [11]. The method is also intended to be used with noisy images. The method performs pixel-by-pixel segmentation taking into account local spatial information. The probability of a pixel belonging to a particular class under spatial constraints is defined as the *a posteriori* spatial probability. The maximum *a posteriori* is then used to classify each pixel.
5. Spatial fuzzy clustering (S-FCM), proposed in [18]. This method is proposed to overcome the problems of standard FCM algorithms when noise and artifacts are present. They incorporate local intensity and spatial information and they can even apply morphological operations and spatial restrictions at a postprocessing stage. In [21], the authors added a level-set step to the method that improves the segmentation. We confine our experiments to the thresholding step, leaving level sets aside.[1]
6. Image thresholding using type II fuzzy sets (FT-II), as proposed in [33]. The method calculates a global threshold by the minimization of a new measure called ultrafuzziness. It considers the threshold as a type II fuzzy set. Only two output regions are considered.

---

[1] The original MATLAB software provided by the authors carries out a Wiener filtering to remove noise form the image. To test the method without any additional filtering, this step has been removed.
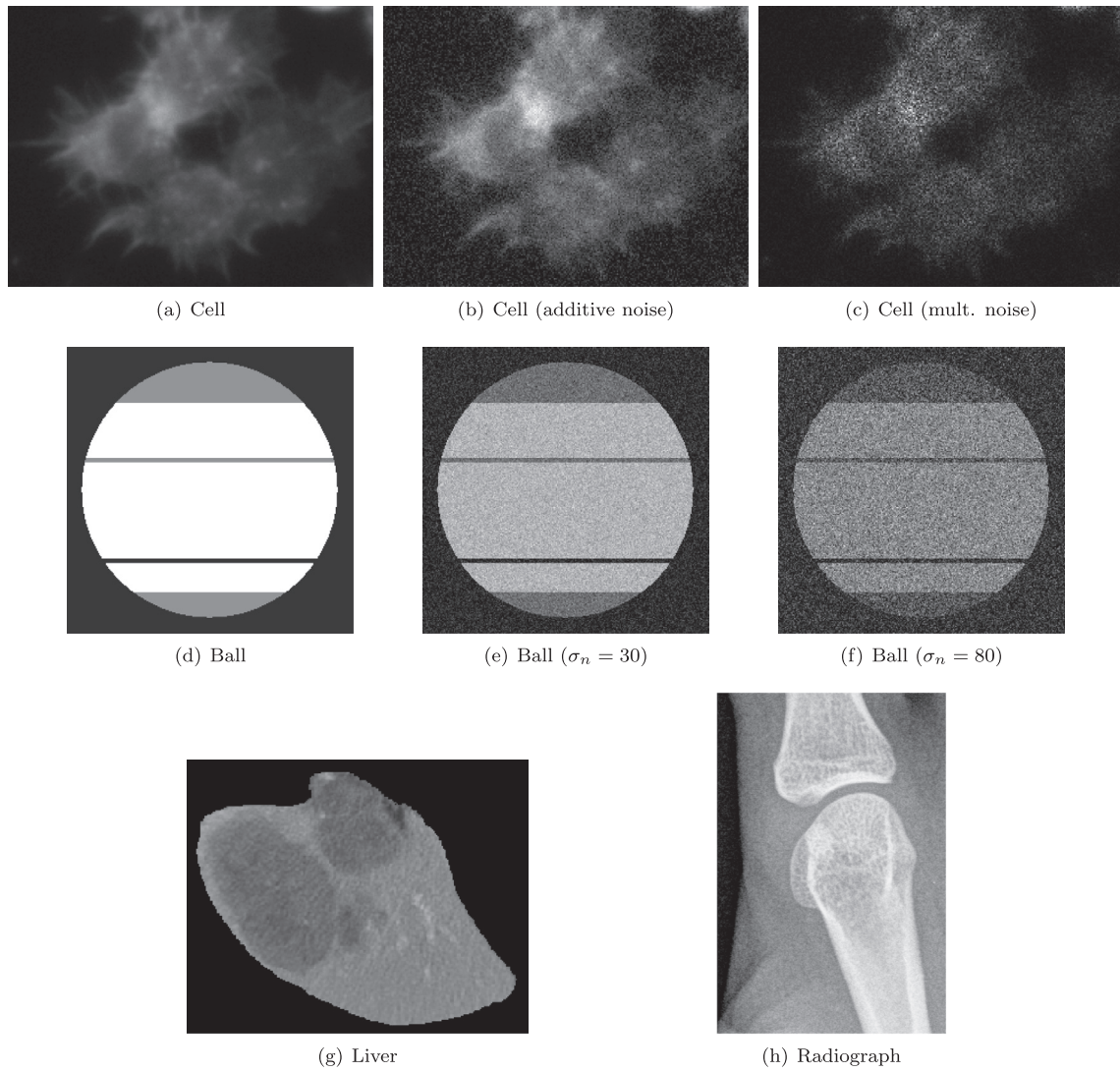
(a) Cell   (b) Cell (additive noise)   (c) Cell (mult. noise)

(d) Ball   (e) Ball ($\sigma_n = 30$)   (f) Ball ($\sigma_n = 80$)

(g) Liver   (h) Radiograph

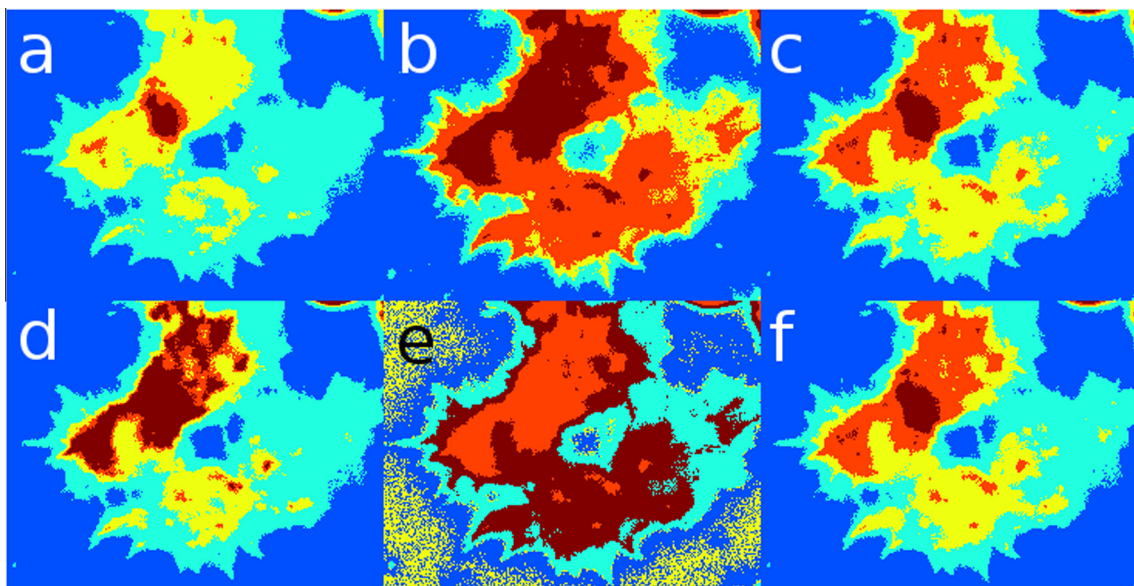**Fig. 4.** Original images used for the experiments.

Fig. 5. Influence of different centroid extraction methods over the final segmentation. (a and d) PTS MF after maxima search; (b and e) Gaussian MF after Gaussian fitting; (c and f) PTS MF after clustering. Top row (a–c) image smoothed with Gaussian kernel. Lower row (d–f) no smoothing.
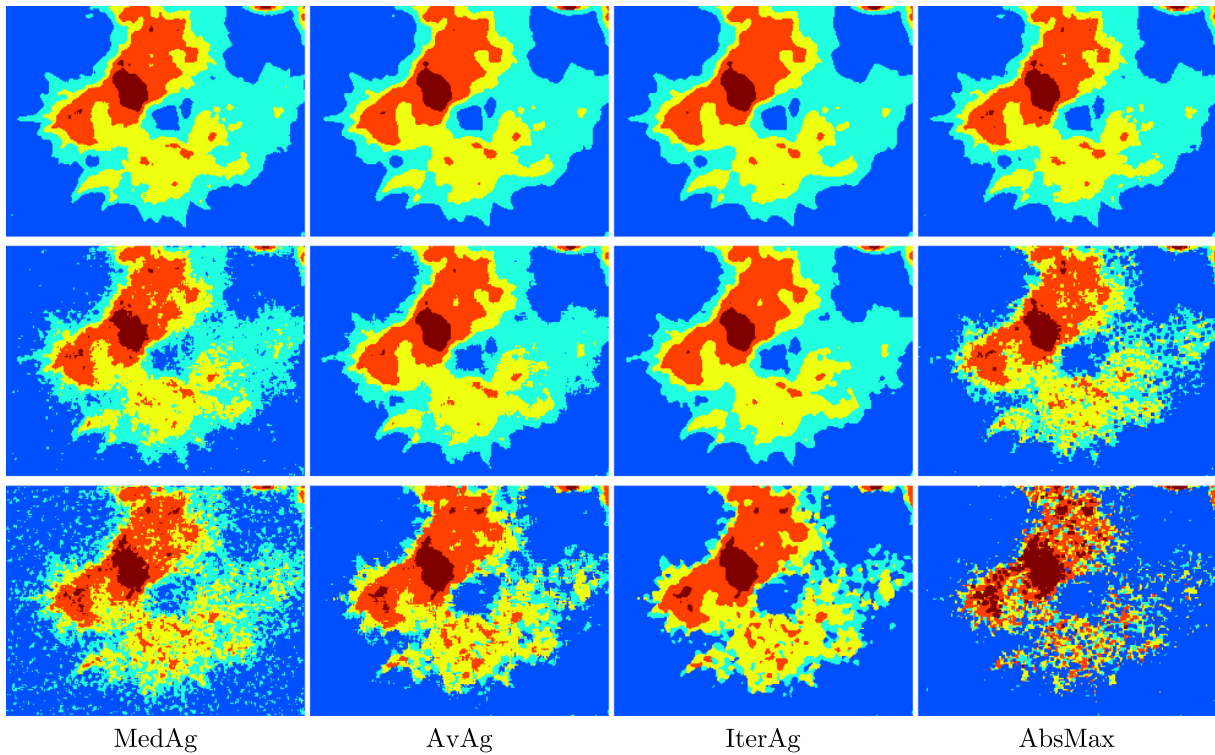
Fig. 6. Comparison of aggregation methods. Top row: original. Middle: additive Gaussian noise ($\sigma = 10$). Bottom: additive Gaussian noise ($\sigma = 20$).
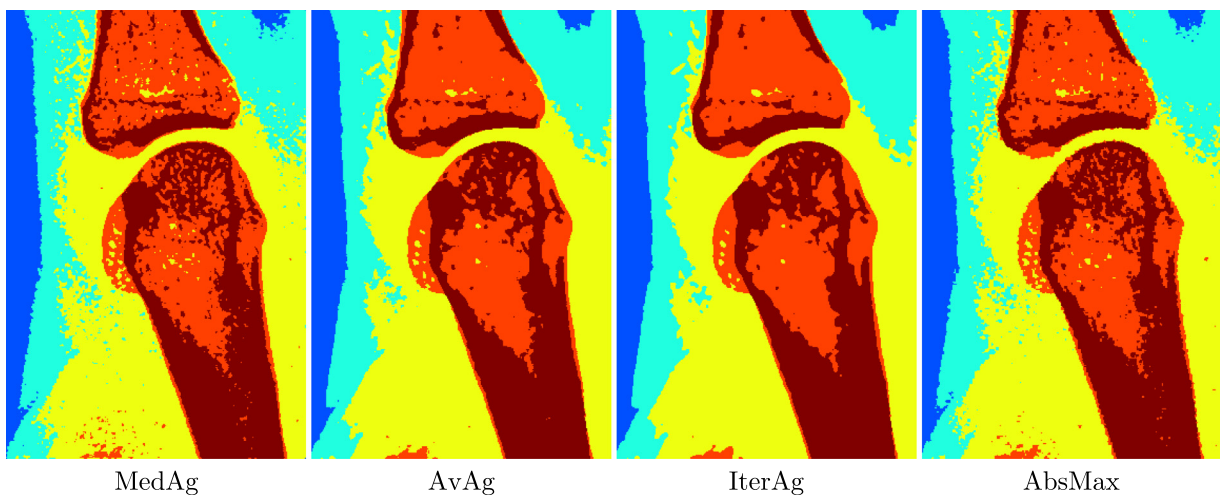

Fig. 7. Comparison of aggregation methods.

We will select three of the proposed aggregation methods, MedAg and AvAg and IterAg, with clustering for centroid selection. For the sake of comparison, the thresholding without aggregation in Eq. (3) is also shown. We will denote it by Max. The following images are used for comparison: the phantom in Fig. 4(d) (corrupted by additive Gaussian noise with $\sigma_n = 30$ and $\sigma_n = 80$), the cell in Fig. 4(a) (original image, a noisy version, corrupted by additive Gaussian noise with $\sigma_n = 10$ and a version corrupted by multiplicative Rayleigh noise) and the liver CT image in Fig. 4(g). For the phantom image, $L = 3$ regions will be considered and for the cell and liver images $L = 5$. Results are shown in Figs. 8 and 9.

Results for the noisy phantom, Fig. 8, show the inability of some of the classical methods to cope with noise in the image. If the behavior of the neighborhood is not taken into account, the variations of

intensity due to noise may be translated into different output regions. This is the case for Otsu-N, FCM and MASP. The 2-region Otsu method and the ITS show good results in preserving the central area as a homogeneous region, although ITS, due to the spatial operations, totally eliminates the inner lines. FT-II shows a more noisy behavior inside the central regions, but the shapes (and in particular the lines) are better defined. A simple median operator may properly fix this result. A better segmentation can be seen in S-FCM for $\sigma = 30$, due to the spatial constraints of this method. However, it cannot cope with high noise levels.

The proposed methods are the ones undoubtedly showing the best results. IterAg of the moderate noise case is able to identify the 3 different regions without any noisy interference. MedAg and AvAg show slightly worse results, but, nevertheless, much
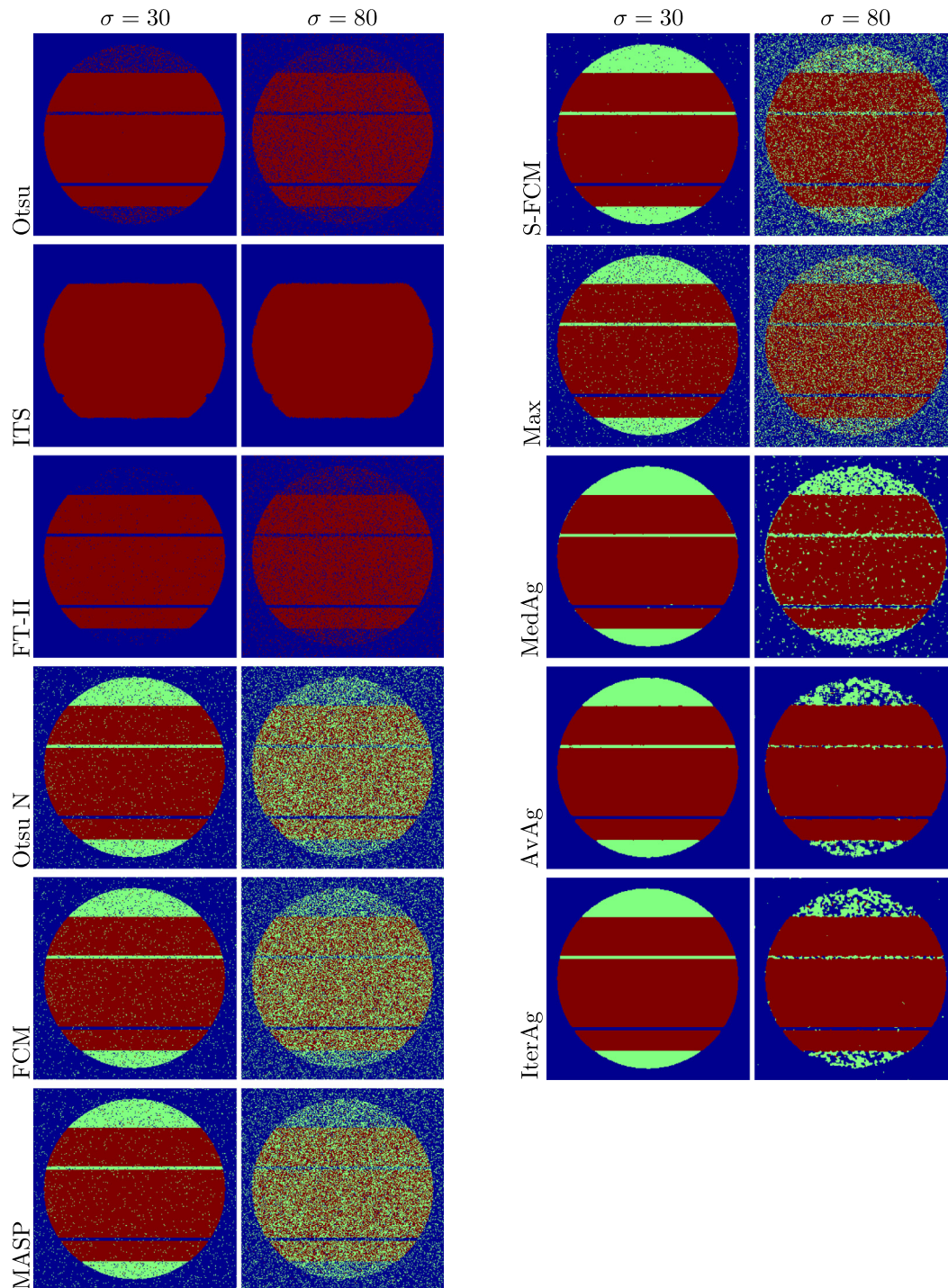
Fig. 8. Comparison of thresholding methods for the phantom corrupted by additive Gaussian noise. Two different levels of noise are considered, $\sigma = 30$ and $\sigma = 80$.

better that the rest. This differences are accentuated when the high noise case is considered. Most of the methods are not able to cope with the pattern, even those that use spatial information, like S-FCM. In those cases, methods based on fuzzy aggregations are the only ones that are able to identify the regions. Even when the segmentation is not totally perfect, AvAg and IterAg succeed in identifying the different areas. The Max results show the thresholding when no aggregation method is used. Note that the noisy pattern present in this image is totally removed by the aggregation methods. It is a clear illustration of the potential of taking into account the neighborhood with a properly tuned fuzzy rule set.

Results for the cell image, Fig. 9, are also illustrative. First, when no noise is added to the image, most of the methods perform similarly, except the ITS that shows a great smoothing. The methods based on fuzzy aggregations show more regular edges and no isolated points, but, nevertheless, results of every method are valid. However, great differences arise when images are corrupted by additive noise. Non-fuzzy techniques show a more noisy pattern and regions are no longer closed and most methods are not able to identify the background. On the other hand, fuzzy methods with aggregations are those with the best results, very similar to the non-noisy case. MedAg still shows some isolated pixels but, again,
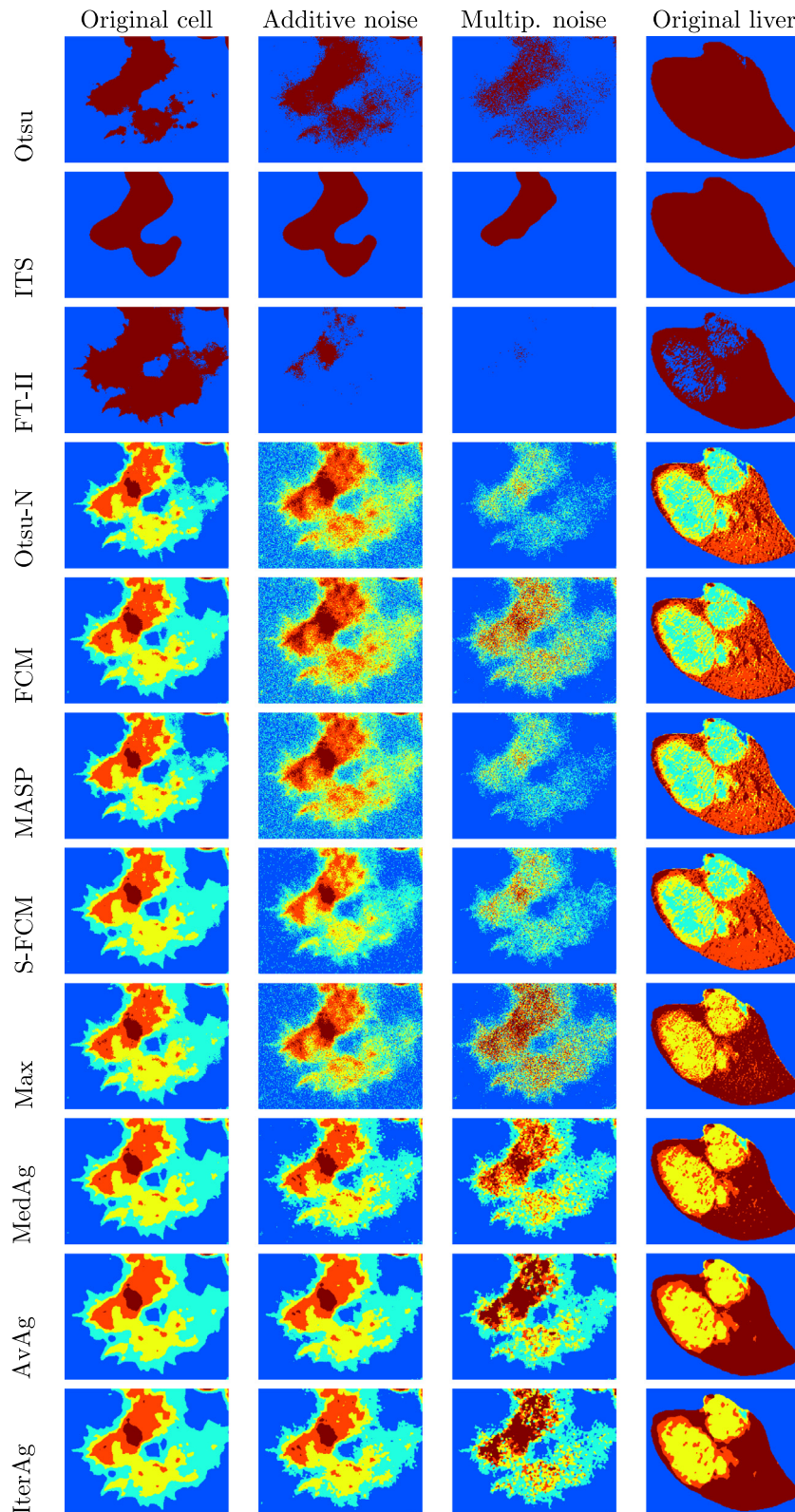
Fig. 9. Comparison of thresholding methods for the cell and liver image.

the three fuzzy methods are able to properly find well-defined closed structures inside the image. These results consistently repeated for multiplicative noise. In that case, the background is easily identified by most of the methods, but the different areas inside the cell are mostly erroneous. The proposed algorithms are the only ones showing a capability of properly identifying these inner areas.

Finally, this behavior is corroborated by results for the liver. Most methods are able to properly identify the different tissues, but the fuzzy aggregations, once more, show more connected results.

Last, for the sake of quantitative comparison, the multilevel thresholding methods are now compared using the Berkeley Segmentation Dataset and Benchmark (BSDS300) [62]. For this experiment, the training set of 200 color images provided by the data base is considered. As ground truth, the BSDS300 provides segmentations of each image carried out by several human subjects. For the sake of simplicity and compatibility with the methods in the literature, all the images have been converted to gray scale. In addition, since the proposed methodology is intended to work in noisy environments, the images have been corrupted with Gaussian noise ($\sigma = 30$) and with multiplicative Rayleigh noise, and the experiment was repeated.

The following scalar measures were considered for region-based comparison:

- *Rand Index (RI):* [63] This is a measure of the similarity between two data clusterings. RI compares the compatibility of assignments between pairs of elements in two clusters by calculating the fraction of correctly classified (respectively misclassified) elements to all elements. For two clusterings $\mathcal{C}_1$ and $\mathcal{C}_2$ it is defined as

$$\mathrm{RI}(\mathcal{C}_1, \mathcal{C}_2) = \frac{2(n_{11} + n_{00})}{N(N-1)} \tag{10}$$

  where N is the total number of points, n_{11} stands for the number of pairs that are in the same cluster in $\mathcal{C}_1$ and $\mathcal{C}_2$, and n_{00} is the number of pairs that are in different clusters. The RI has a value between 0 and 1, with 0 indicating that the two data clusters do not agree on any pair of points and 1 indicating that the data clusters are exactly the same.

- *Variation of Information (VI):* [64] This measures the distance between two segmentations in terms of their average conditional entropy given by:

$$\mathrm{VI}(\mathcal{C}_1, \mathcal{C}_2) = \mathcal{H}(\mathcal{C}_1) + \mathcal{H}(\mathcal{C}_2) - 2\mathcal{I}(\mathcal{C}_1, \mathcal{C}_2) \tag{11}$$

  where $\mathcal{H}(\mathcal{C}_i)$ is the entropy associated with clustering $\mathcal{C}_i$ and $\mathcal{I}$ is the mutual information between two clusterings $\mathcal{C}_1$ and $\mathcal{C}_2$.

- *The covering* of a segmentation $\mathcal{S}_1$ by segmentation $\mathcal{S}_2$ as defined in [65]:

$$\mathcal{C}(\mathcal{S}_2 \to \mathcal{S}_1) = \frac{1}{N} \sum_{\mathcal{R}_1 \in \mathcal{S}_1} |\mathcal{R}_1| \max_{\mathcal{R}_2 \in \mathcal{S}_2} \mathcal{O}(\mathcal{R}_1, \mathcal{R}_2) \tag{12}$$

  where $\mathcal{O}(\mathcal{R}_1, \mathcal{R}_2)$ is the overlap between regions $\mathcal{R}_1$ and $\mathcal{R}_2$ defined as:

$$\mathcal{O}(\mathcal{R}_1, \mathcal{R}_2) = \frac{|\mathcal{R}_1 \cap \mathcal{R}_2|}{|\mathcal{R}_1 \cup \mathcal{R}_2|} \tag{13}$$

We will use two complementary descriptors, $\mathcal{C}(\mathcal{S}_2 \to \mathcal{S}_1)$ and $\mathcal{C}(\mathcal{S}_1 \to \mathcal{S}_2)$.

For each method and for each image, we consider different segmentations using 3–10 regions. The best match, in terms of best benchmark results, is considered. Results are shown in Table 1. Note that, for RI and the overlap measures, the greater the better, while for VI the smaller the better. The best value for each row is highlighted.

Results show that the proposed methods are those with the best values on the four considered measures. What is more, they also show a great robustness when the noise experiments are carried out. Note, for instance, the small variability of the results for the overlap measures in IterAg when compared with other thresholding methods.

4. Conclusions

We have presented a new thresholding methodology. This methodology overcomes some of the common drawbacks of thresholding methods when images are corrupted with artifacts and noise. It is related to published spatial-based thresholding methods, but it also presents some important differences from them, being also related to fuzzy-based strategies. The philosophy behind the proposed methodology is simple: in noisy images the intensity value of a pixel should not be an absolute classification feature, since noise will generate similar intensity levels in different objects, leading to a misclassification of isolated pixels. Instead, some metric based on the intensity levels must be considered and this metric must be weighted by the information of the surrounding pixels. For this task we have proposed the use of fuzzy membership degrees. Thus, each pixel will belong to different output classes with a certain degree. This fuzzy membership could also be replaced by distance to centroids, for instance. The key of the method is to work in the membership *space* rather than on the image space. This way, the memberships of the pixels in a local neighborhood modify the membership degree of every particular pixel.

The whole process presented here should be seen as a methodology rather than a closed algorithm, and each of the different steps can be replaced by equivalent operations. The starting point is the definition of the centroids for the output classes. In the experiments section we chose to use an FCM algorithm for its robustness and good results. The purpose of this step is to achieve well defined output centroids, and other FCM algorithms have also achieved excellent results, as in [19,20,18]. Alternatively most of the thresholding and clustering methods in the literature can be used to carry out this task, so we can benefit from very accurate optimization methods that have been used for many years.

The key of the proposal is the use of the spatial aggregation step, which makes our method able to overcome noise-related problems that traditional methods cannot cope with. Our first

Table 1
Region benchmarks on the BSDS300. Three experiments are considered: (1) Original data base; (2) Corrupted by Gaussian noise; (3) Corrupted with multiplicative Rayleigh noise. For each configuration, the best value is highlighted.

		Otsu-N	FCM	S-FCM	MASP	MedAg	AvAg	IterAg
RI	Original	0.7138	0.7161	0.7179	0.6721	0.7198	0.7237	**0.7241**
	Gaussian	0.6816	0.6862	0.6902	0.6425	**0.7075**	0.7026	0.7029
	Rayleigh	0.6325	0.6704	0.6598	0.5803	**0.6918**	0.6538	0.6502
VI	Original	2.9746	2.9914	2.9221	3.4835	2.9483	2.8912	**2.8820**
	Gaussian	3.3867	3.3964	3.2193	3.9674	3.0776	2.9473	**2.9216**
	Rayleigh	3.4821	3.5300	3.2588	3.8401	3.2903	2.9911	**2.931**
$\mathcal{C}(\mathcal{S}_2 \to \mathcal{S}_1)$	Original	0.3535	0.3499	0.3602	0.2943	0.3558	0.3644	**0.3658**
	Gaussian	0.2862	0.2845	0.3121	0.2305	0.3331	0.3517	**0.3552**
	Rayleigh	0.2557	0.2506	0.2765	0.2251	0.2951	0.3332	**0.3400**
$\mathcal{C}(\mathcal{S}_1 \to \mathcal{S}_2)$	Original	0.4414	0.4365	0.4503	0.3414	0.4424	0.4493	**0.4507**
	Gaussian	0.3638	0.3614	0.3960	0.2662	0.4191	0.4447	**0.4480**
	Rayleigh	0.3526	0.3437	0.3935	0.2933	0.3816	0.4438	**0.4554**

attempts to define general purpose thresholding aggregations have shown good results, and can potentially get even better when applied with constraints suitable for particular segmentation goals.

All in all, the methodology proposed has the following advantages: (1) It is totally automatic, and does not require human intervention; (2) the hard thresholding decision is postponed to the final stage, so all the spatial operations are done before taking into account the different memberships; (3) spatial aggregations make the thresholding more robust to noise and artifacts; (4) it can benefit from the use of accurate thresholding methods in the first step; and (5) the spatial aggregations can be specifically designed for a particular application, and heuristic information can be added via a fuzzy inference rule base.

Acknowledgements

Appendix A. Supplementary data

Supplementary data associated with this article can be found, in the online version, at http://dx.doi.org/10.1016/j.knosys.2015.02.029.

References

[1] S. Taheri, S. Ong, V. Chong, Level-set segmentation of brain tumors using a threshold-based speed function, Image Vis. Comput. 28 (1) (2010) 26–37.
[2] D. Mukherjee, N. Ray, S. Acton, Level set analysis for leukocyte detection and tracking, IEEE Trans. Image Proccess. 13 (4) (2004) 562–572.
[3] J. Sijbers, A. Postnov, Reduction of ring artefacts in high resolution micro-CT reconstructions, Phys. Med. Biol. 49 (14) (2004) 247.
[4] P.L. Rosin, Thresholding for change detection, Comput. Vis. Image Understanding 86 (2) (2002) 79–95.
[5] P.L. Rosin, E. Ioannidis, Evaluation of global image thresholding for change detection, Pattern Recogn. Lett. 24 (14) (2003) 2345–2356.
[6] G. Vegas-Sánchez-Ferrero, S. Aja-Fernández, C. Palencia, M. Martin-Fernandez, A generalized gamma mixture model for ultrasonic tissue characterization, Comput. Math. Methods Med. (2012).
[7] N. Otsu, A threshold selection method from gray-scale histogram, IEEE Trans. Syst., Man and Cyb. 9 (1) (1979) 62–66.
[8] T. Kurita, N. Otsu, N. Abdelmalek, Maximum likelihood thresholding based on population mixture models, Pattern Recogn. 25 (10) (1992) 1231–1240.
[9] M. Sezgin, B. Sankur, Survey over image thresholding techniques and quantitative performance evaluation, J. Electron. Imaging 13 (1) (2004) 146–165.
[10] H. Wu, J. Barba, J. Gil, Iterative thresholding for segmentation of cells from noisy images, J. Microsc. 197 (3) (2000) 296–304.
[11] C. Leung, F. Lam, Maximum a posteriori spatial probability segmentation, IEE Proc. – Vis., Image Signal Process. 144 (3) (1997) 161–167.
[12] P.K. Sahoo, S. Soltani, A.K.C. Wong, A survey of thresholding techniques, Comput. Vis., Graphics, Image Process. 41 (2) (1988) 233–260.
[13] R.C. González, R.E. Woods, Digital Image Processing, Addision Wesley, 1992.
[14] L. Mahmoudi, A. El Zaart, A survey of entropy image thresholding techniques, in: Advances in Computational Tools for Engineering Applications (ACTEA), 2012 2nd International Conference on, IEEE, 2012, pp. 204–209.
[15] S.U. Lee, S. Yoon Chung, R.H. Park, A comparative performance study of several global thresholding techniques for segmentation, Comput. Vis., Graphics, Image Process. 52 (2) (1990) 171–190.
[16] F.R.D. Velasco, Thresholding using the isodata clustering algorithm, IEEE Trans., Man Cyber. SMC-10 (1980) 771–774.
[17] H. Lee, R.H. Park, Comments on an optimal threshold scheme for image segmentation, IEEE Trans. Syst., Man Cyber. SMC-20 (1990) 741–742.
[18] W. Cai, S. Chen, D. Zhang, Fast and robust fuzzy c-means clustering algorithms incorporating local information for image segmentation, Pattern Recogn. 40 (3) (2007) 825–838.
[19] Y. Yong, Z. Chongxun, L. Pan, A novel fuzzy c-means clustering algorithm for image thresholding, Meas. Sci. Rev. 4 (1) (2004) 11–19.
[20] A. Masood, Al-Jumaily, A. Ali, Fuzzy c mean thresholding based level set for automated segmentation of skin lesions, J. Signal Inform. Process. 4 (2013) 66.
[21] B.N. Li, C.K. Chui, S. Chang, S.H. Ong, Integrating spatial fuzzy clustering with level set methods for automated medical image segmentation, Comput. Biol. Med. 41 (1) (2011) 1–10.
[22] T. Pun, A new method for gray-level picture threshold using the entropy of the histogram, Signal Proccess. 23 (1980) 223–237.
[23] T. Pun, Entropic thresholding: a new approach, Comput. Graphics Image Process. 16 (1981) 210–239.
[24] J.N. Kapur, P.K. Sahoo, A.K.C. Wong, A new method for gray-level picture thresholding using the entropy of the histogram, Comput. Vis., Graphics, Image Process. 29 (1985) 273–285.
[25] L. Hertz, R.W. Schafer, Multilevel thresholding using edge matching, Comput. Vis. Graph. Image Process. 44 (1988) 279–295.
[26] L. O'Gorman, Binarization and multithresholding of document images using connectivity, Graphical Models Image Process. 56 (1994) 494–506.
[27] S.K. Pal, R.A. King, A.A. Hashim, Automatic gray level thresholding through index of fuzziness and entropy, Pattern Recogn. Lett. 1 (1980) 141–146.
[28] C.A. Murthy, S.K. Pal, Fuzzy thresholding: a mathematical framework, bound functions and weighted moving average technique, Pattern Recogn. Lett. 11 (1990) 197–206.
[29] K. Ramar, S. Arunigam, S.N. Sivanandam, L. Ganesan, D. Manimegalai, Quantitative fuzzy measures for threshold selection, Pattern Recogn. Lett. 21 (2000) 1–7.
[30] O.J. Tobias, R. Seara, Image segmentation by histogram thresholding using fuzzy sets, IEEE Trans. Image Proccess. 11 (12) (2002) 1457–1465.
[31] M. Forero, Fuzzy thresholding and histogram analysis, in: M. Nachtegael, D. Van der Weken, D. Van de Ville, E. Kerre (Eds.), Fuzzy Filters for Image Processing, Springer, Berlin, 2003, pp. 129–152.
[32] A.Z. Arifin, A.F. Heddyanna, H. Studiawan, Ultrafuzziness optimization based on type ii fuzzy sets for image thresholding, ITB J. Inform. Commun. Technol. 4 (2) (2010) 79–94.
[33] H.R. Tizhoosh, Image thresholding using type II fuzzy sets, Pattern Recogn. 38 (12) (2005) 2363–2372.
[34] J.M. Mendel, Fuzzy logic systems for engineering: a tutorial, Proc. IEEE 83 (3) (1995) 345–377.
[35] H.R. Berenji, Fuzzy Logic Controllers: An Introduction to Fuzzy Logic Applications and Intelligent Systems, Kluwer Academic Publisher, Boston, Mass, 1992.
[36] P. Szczepaniak, G.L.P.J, J. Kacprzyk (Eds.), Fuzzy Systems in Medicine, Physica-Verlag, New York, 2000.
[37] E. Kerre, M. Nachtegael (Eds.), Fuzzy Techniques in Image Processing, Physica-Verlag, New York, 2000.
[38] D. Van De Ville, M. Nachtegael, D. Van der Weken, E. Kerre, W. Philips, I. Lemahieu, Noise reduction by fuzzy image filtering, IEEE Trans. Fuzzy Syst. 11 (4) (2003) 429–436.
[39] L. Garmendia, The evolution of the concept of fuzzy measure, in: Intelligent Data Mining, Springer, 2005, pp. 185–200.
[40] M. Larbani, C.-Y. Huang, G.-H. Tzeng, A novel method for fuzzy measure identification, Int. J. Fuzzy Syst. 13 (1) (2011) 24–34.
[41] C. Jawahar, P.K. Biswas, A. Ray, Investigations on fuzzy thresholding based on fuzzy clustering, Pattern Recogn. 30 (10) (1997) 1605–1613.
[42] N. Ramesh, J.-H. Yoo, I. Sethi, Thresholding based on histogram approximation, IEE Proc. – Vis., Image Signal Process. 142 (5) (1995) 271–279.
[43] L.-K. Huang, M.-J.J. Wang, Image thresholding by minimizing the measures of fuzziness, Pattern Recogn. 28 (1) (1995) 41–51.
[44] M.S. Prasad, T. Divakar, B.S. Rao, N. Raju, Unsupervised image thresholding using fuzzy measures, Int. J. Comput. Appl. 27 (2) (2011) 32–41.
[45] S.K. Pal, A. Rosenfeld, Image enhancement and thresholding by optimization of fuzzy compactness, Pattern Recogn. Lett. 7 (1988) 77–86.
[46] S. Di Zenzo, L. Cinque, S. Levialdi, Image thresholding using fuzzy entropies, IEEE Trans. Syst., Man, Cybern., Part B: Cybern. 28 (1) (1998) 15–23.
[47] B. Akay, A study on particle swarm optimization and artificial bee colony algorithms for multilevel thresholding, Appl. Soft Comput. 13 (6) (2013) 3066–3091.
[48] P. Sathya, R. Kayalvizhi, Modified bacterial foraging algorithm based multilevel thresholding for image segmentation, Eng. Appl. Artif. Intell. 24 (4) (2011) 595–615.
[49] M.-H. Horng, Multilevel minimum cross entropy threshold selection based on the honey bee mating optimization, Expert Syst. Appl. 37 (6) (2010) 4580–4592.
[50] J. Bezdek, FCM: the fuzzy c-means clustering algorithm, Comput. Geosci. 10 (1984) 191–203.
[51] D. Drumheller, General expressions for Rician density and distribution functions, IEEE Trans. Aerospace Electron. Syst. 29 (2) (1993) 580–588.
[52] H. Gudbjartsson, S. Patz, The Rician distribution of noisy MRI data, Magn. Reson. Med. 34 (6) (1995) 910–914.
[53] G. Vegas-Sanchez-Ferrero, D. Martín-Martinez, S. Aja-Fernández, C. Palencia, On the influence of interpolation on probabilistic models for ultrasonic images, in: Proc. of the ISBI, Rotterdam, Netherlands, 2010, pp. 292–295.
[54] X. Zeng, M. Singh, Approximation theory of fuzzy systems – SISO case, IEEE Trans. Fuzzy Sys. 2 (2) (1994) 162–176.

[55] S. Aja-Fernández, C. Alberola-López, G. Cybenko, A fuzzy MHT algorithm applied to text-based information tracking, IEEE Trans. Fuzzy Syst. 10 (3) (2002) 360–374.

[56] B. Devi, V. Sarma, Estimation of fuzzy memberships from histograms, Inform. Sci. 35 (1) (1985) 43–59.

[57] A. Gillet, L. Macaire, C. Botte-Lecocq, J.-G. Postaire, Color image segmentation by analysis of 3d histogram with fuzzy morphological filters, in: M. Nachtegael, D. Van der Weken, E. Kerre, D. Van De Ville (Eds.), Fuzzy Filters for Image Processing, Studies in Fuzziness and Soft Computing, vol. 122, Springer, Berlin, Heidelberg, 2003, pp. 153–177.

[58] C.-C. Yang, N. Bose, Generating fuzzy membership function with self-organizing feature map, Pattern Recogn. Lett. 27 (5) (2006) 356–365.

[59] F. Russo, {FIRE} operators for image processing, Fuzzy Sets Syst. 103 (2) (1999) 265–275.

[60] H. Tizhoosh, Fast fuzzy edge detection, in: Fuzzy Information Processing Society, 2002. Proceedings. NAFIPS. 2002 Annual Meeting of the North American, 2002, pp. 239–242.

[61] K.-S. Chuang, H.-L. Tzeng, S. Chen, J. Wu, T.-J. Chen, Fuzzy c-means clustering with spatial information for image segmentation, Comput. Med. Imag. Graphics 30 (1) (2006) 9–15.

[62] D. Martin, C. Fowlkes, D. Tal, J. Malik, A database of human segmented natural images and its application to evaluating segmentation algorithms and measuring ecological statistics, in: Proc. 8th Int'l. Conf. Computer Vision, vol. 2, 2001, pp. 416–423.

[63] W.M. Rand, Objective criteria for the evaluation of clustering methods, J. Am. Stat. Assoc. 66 (1971) 846–850.

[64] M. Meilă, Comparing clusterings: an axiomatic view, in: Proc. of the 22nd International Conference on Machine Learning, New York, NY, USA, 2005, pp. 577–584.

[65] P. Arbeláez, M. Maire, C. Fowlkes, J. Malik, Contour detection and hierarchical image segmentation, IEEE Trans. Pattern Anal. Mach. Intell. 33 (5) (2011) 898–916.